First Isotopic Age Constraints for the Dean River Metamorphic Belt, Anahim Lake area: Implications for Crustal Extension and Resource Evaluation in West-Central British Columbia

by M.G. Mihalynuk and R.M. Friedman[1]

KEYWORDS: isotopic dating, Dean River metamorphic belt, Anahim Lake geology, Tatla Lake Metamorphic Complex, detachment mineralization, polymetallic fault-related, deposit model

INTRODUCTION

Reconnaissance field studies conducted as part of the Beetle Impacted Zone project included investigation of the Dean River metamorphic belt in northwestern Anahim Lake map area (Figure 1; for an introduction to the Beetle Impacted Zone project (BIZ), its mandate and deliverables to date, *see* Mihalynuk, 2007a, b and Mihalynuk et al., 2007, 2008, 2009). Aims of the reconnaissance investigation were: to ascertain the type of protoliths and their geological setting, evaluate their mineral resource potential and establish the nature of the basal contact and pre-Miocene topography. We collected samples for isotopic age determination as an aid to correlation with rock packages for which the mineral potential is more clearly understood. Based on MINFILE records, (MINFILE, 2008), no mineral occurrences or mineral tenures are currently known to exist within the Dean River metamorphic belt (DRMB). We present the age data here together with field and microscopic observations, which support a correlation with rocks in the Tatla Lake Metamorphic Complex.

LOCATION

Rocks of the Dean River metamorphic belt are shown by Schiarizza et al. (1994) to extend from Lily Lake near Ulkatcho to the headwaters of Puntzi Creek near Chantslar Lake (northwestern to south-central Anahim Lake map area, NTS 093C; Figure 1). This area corresponds largely with the eastern headwaters of the Dean River. Fieldwork was focused on a broad area of discontinuous exposure near Rainbow Lake, 45 km north of Anahim Lake. The main Dean River forest service road, which originates at the northern outskirts of Anahim Lake village, provides access to the area. A subsidiary logging road departs from the main road between Far and Tanswanket creeks and DRMB rocks are exposed in the roadbed within a kilometre of the Tanswanket Creek crossing. Fieldwork in this area was aided by lack of undergrowth due to a forest fire in the summer of 2006 (Figure 2).

GEOLOGICAL SETTING AND PREVIOUS WORK

Little is known about the DRMB other than its regional distribution as compiled by Schiarizza et al. (1994), which is mainly based upon regional mapping by Tipper (1969). Tipper included rocks of the DRMB in his "Unit 4…mainly gneisses that occur in a belt northeast of the Coast Mountains and can be traced 40 miles to the northwest and more than 60 miles southeast". At its southern limit, Unit 4 included parts of the Tatla Lake Metamorphic Complex (TLMC; Friedman, 1988). In observance of the limits of the TLMC mapped by Friedman (1988), Schiarizza et al. (1994) sought to distinguish the northern continuation of Tipper's northwest-trending belt of metamorphic rocks, and named them the 'Dean River metamorphic belt' (Figure 2). In a study aimed at the Miocene and younger volcanic rocks of the Ilgachuz Range, Souther and Souther (1994) extended the TLMC to include DRMB rocks near Rainbow Lake. Souther and Souther showed that, like the TLMC along strike to the southeast, these rocks display a dominantly east-striking foliation and a contact with presumably less deformed Early Jurassic Hazelton Group volcanic rocks, which are obscured by glacial cover.

SAMPLE DESCRIPTIONS

Dean River metamorphic belt rocks in the Rainbow Lake area include dacite, tonalite, mafic tuff and volcanic metasediment. All display evidence of at least two phases of deformation, typically a mylonitic foliation which is crenulated and locally overprinted by a late mylonitic fabric.

Dacite occurs as low, glaciated, slabby or blocky, light grey to white outcrops. Protolith textures are common in all but the most intensely mylonitized rocks. Relict flattened crystal-rich clasts are interpreted as lapilli, but they could be a product of attenuated and dismembered dikelets. A lapilli clast origin is preferred as crystal fragments (relict, not cataclastic) and embayed quartz eyes are common (Figure 3). Typical porphyroclasts include medium-grained plagioclase (~15%, and probably minor sanidine), quartz eyes (~5%), and sparse remnants of biotite (<1%), which can be difficult to distinguish from secondary biotite. The predominant secondary minerals are fine- to medium-grained muscovite, which may account for 25% of the rock, and fine-grained secondary calcite (up to 10%). Much of the rock consists of comminuted quartz and feldspar. Shear

[1] *Pacific Centre for Isotopic and Geochemical Research, University of British Columbia, Vancouver, BC*

This publication is also available, free of charge, as colour digital files in Adobe Acrobat® PDF format from the BC Ministry of Energy, Mines and Petroleum Resources website at http://www.empr.gov.bc.ca/Mining/Geoscience/PublicationsCatalogue/Fieldwork/Pages/default.aspx.

sense indicators include rotated feldspar porphyroclasts and incipiently developed S-C fabrics (Figure 4), but variations in the sense of offset are suggestive of folded shear zone boundaries.

ISOTOPIC AGE DETERMINATION

Three samples of the dacite unit were selected for isotopic age determination. One of the least deformed and least metamorphosed outcrops was sampled for U-Pb age determination. A strongly schistose and white mica-rich sample and a late (Figure 5), relatively undeformed quartz-

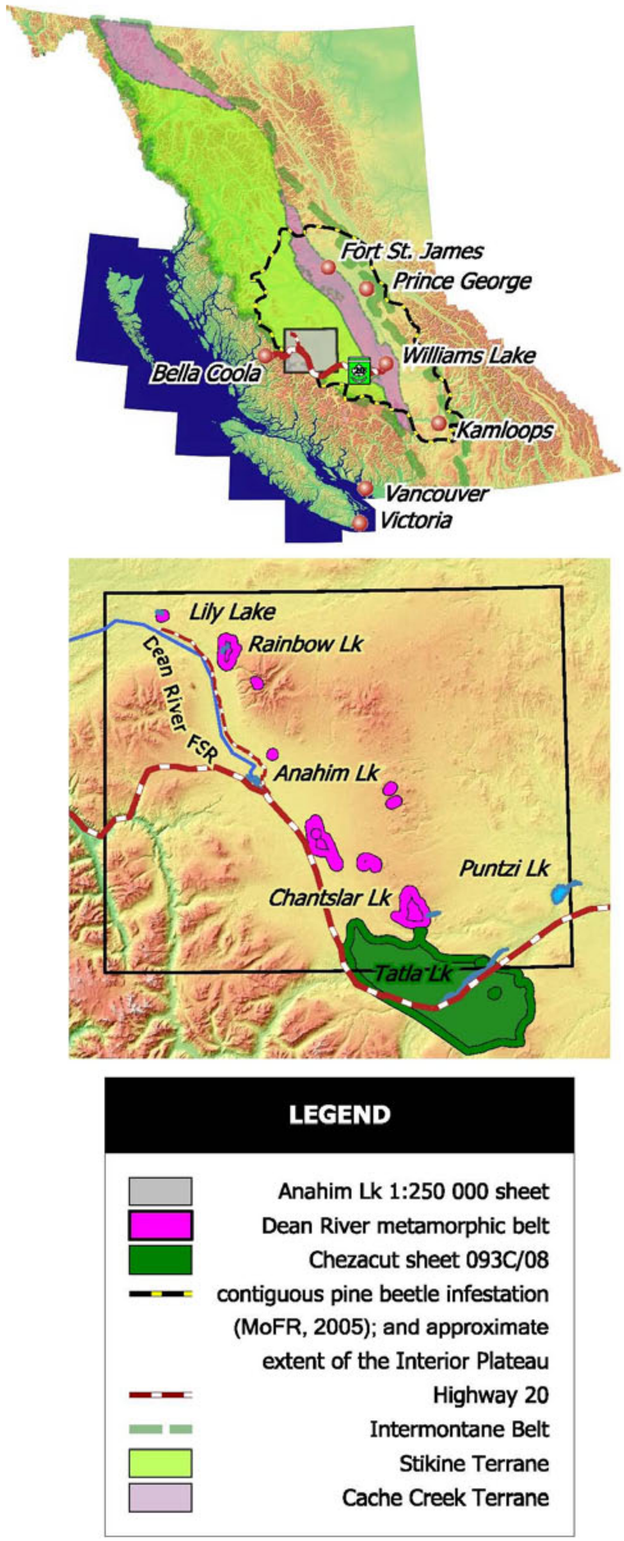

Figure 1. Location map showing the Interior Plateau, Beetle Impacted Zone, Intermontane Belt and constituent terranes. Magnified Anahim Lake inset shows the Tatla Lake Metamorphic Complex, Dean River metamorphic belt and geographic features mentioned in the text.

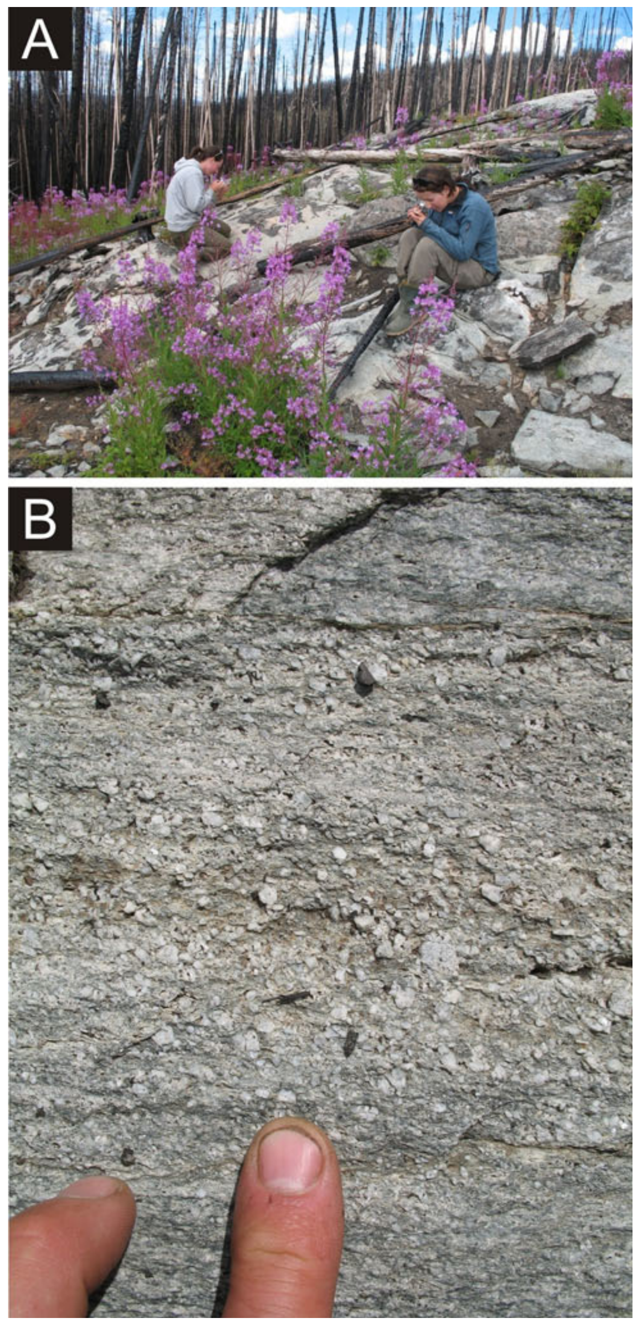

Figure 2. a) General nature of the outcrop shown in this 2006 photo (view ~north). **b)** Close-up view of typical fragmented crystal-rich dacite, like that sampled for U-Pb isotopic age determination.

feldspar segregation (Figure 4c) were sampled for $^{40}Ar/^{39}Ar$ age determination.

All sample preparation and analytical work for the U-Pb and $^{40}Ar/^{39}Ar$ isotopic ages presented here was conducted at the Pacific Centre for Isotopic and Geochemical Research (PCIGR) at the Department of Earth and Ocean Sciences, University of British Columbia.

The U-Pb isotopic age determinations reported here were acquired by thermal ionization mass spectroscopy (U-Pb TIMS). The $^{40}Ar/^{39}Ar$ isotopic age determinations were

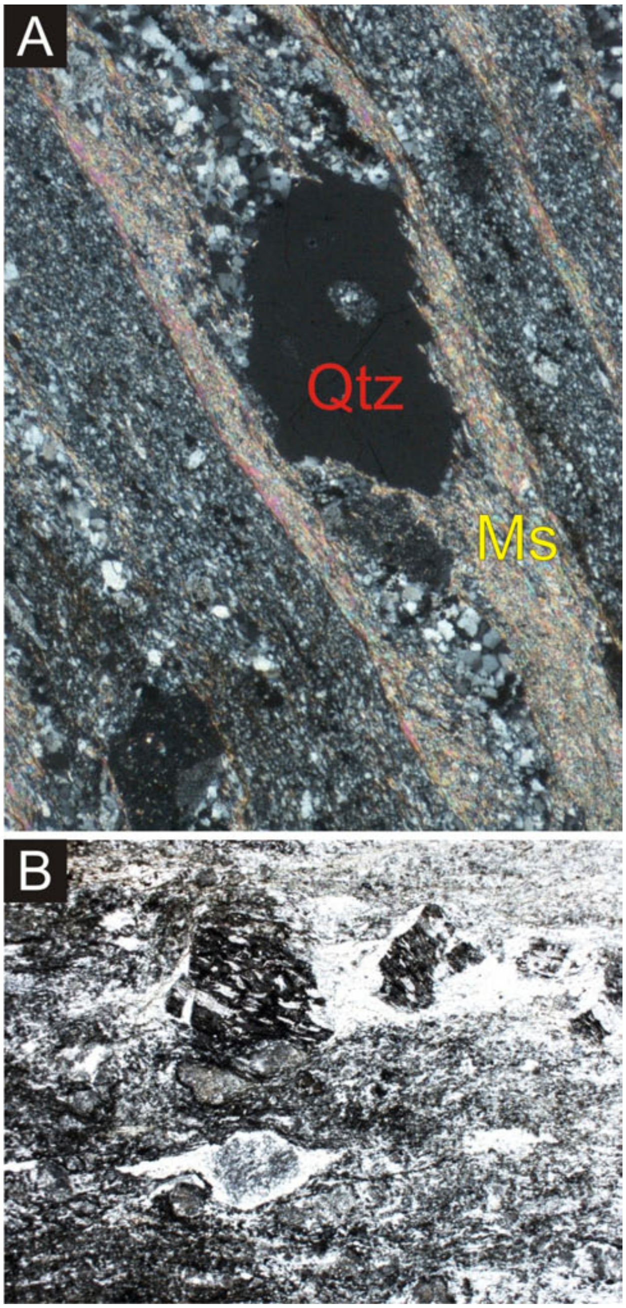

Figure 3. Photomicrographs of **a)** embayed quartz (Qtz) and muscovite (Ms) concentrated along folia in strongly foliated dacite such as that sampled for $^{40}Ar/^{39}Ar$ age determination; **b)** fragmented and rotated trachytic volcanic granules in sedimentary unit display pressure shadows. Long dimensions of photos represent 2.5 and 5 mm, respectively.

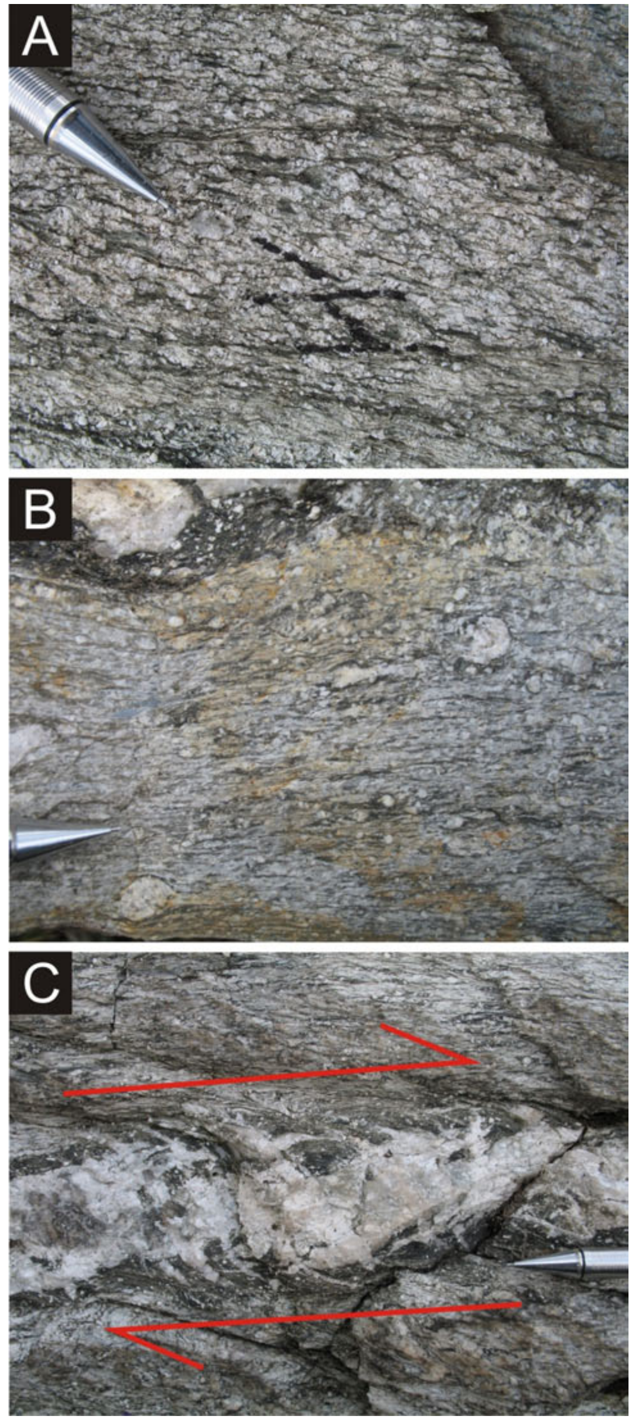

Figure 4. Outcrops displaying shear sense indicators: **a)** foliated, white mica-rich part of the unit and S-C developed within moderately foliated dacite, **b)** strong S2 (crenulation cleavage) developed with preserved porphyroclasts displaying mainly dextral shear sense, although one -type porphyroclast (below pencil tip) appears to display sinistral shear sense (mineral elongation is within the fabric plane and ~ parallel to outcrop surface in both a) and b); **c)** relatively undeformed quartz-feldspar segregation (sampled for $^{40}Ar/^{39}Ar$ age determination without success) within a brittle sigmoid shear zone (dextral shear sense indicated).

acquired by the laser-induced step-heating technique. Details of the both analytical techniques are presented in Logan et al. (2007).

U-Pb protolith age

Zircon was separated from dacite sample MMI07-33-3 using standard mineral separation techniques (crushing, grinding, Wilfley [wet shaker] table, heavy liquids and magnetic separation), followed by hand picking. Five air-abraded single zircon grains were analyzed with results plotted in Figure 6 and listed in Table 1. All data overlap concordia at the 2 confidence level. Dispersion of Pb-U dates are attributed to minor Pb loss; the weighted average of overlapping ^{206}Pb-^{238}U dates for older grains A and B at 150.2 ±0.3 Ma is taken as the best estimate for the age of the rock (Figure 7). However, because zircons were only air abraded (not chemically abraded), Pb loss for grains A and B cannot be ruled out and this estimate should be considered as a minimum age. The weighted average of ^{207}Pb-^{206}Pb dates for all analyzed grains at ca. 153 Ma gives a rough measure of the maximum age allowed with the current data set. We will refine the age of this rock by analyzing several zircon grains that have undergone chemical abrasion pre-treatment (Mundil et al., 2004; Mattinson, 2005).

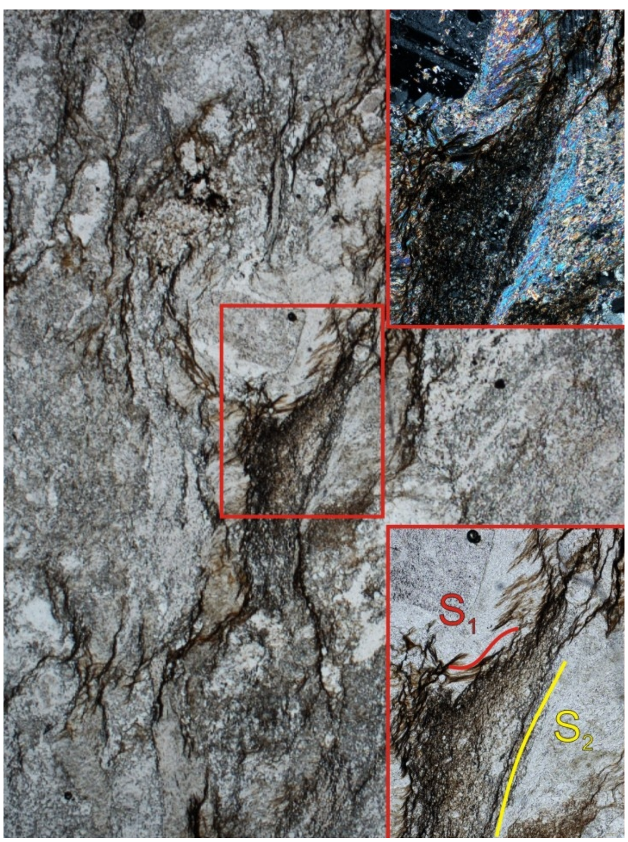

Figure 5. Photomicrograph of Dean River metamorphic belt dacite showing plagioclase porphyroclast and higher magnification inset in both plane polarized (bottom right) and cross polarized light (top right). Note abundant muscovite with high birefringence. Long dimension of photo represents ~5 mm.

^{40}Ar/^{39}Ar cooling age

No useful data was acquired from the sample of syn- to post-kinematic quartz-feldspar segregation, probably because the feldspar was albite and not sufficiently K-rich. The white mica sample did yield useful results, although the release spectrum was plagued by excess argon (Figure 8) as indicated by the rising steps within the spectrum. Excess argon is present when the initial ^{40}Ar/^{36}Ar value is >295.5 Ma (Table 2). This condition is mitigated by the isochron plots shown in Figure 9a, b, which produce reliable cooling ages of 49.9 ±0.5 Ma.

REGIONAL CORRELATION AND IMPLICATIONS

Protoliths and structural fabrics within the DRMB are similar to those within the ductilely sheared assemblage of the TLMC. We suggest that the instincts of Tipper (1969) and Souther and Souther (1994) led them to correctly correlate metamorphic rocks in northwestern through south-central Anahim Lake area. That the TLMC is more extensive than originally mapped by Friedman (1988) is not surprising given that his limits of the TLMC were governed in large part by the extent of his map coverage. Furthermore, Friedman and Armstrong (1988) hypothesized a crustal-scale shear zone linking core complexes on both sides of the Intermontane Belt (Figure 1); such a shear zone may also provide a linkage between intracontinental transform faults (Struik, 1993). If correct, a more widespread manifestation of the crustal-scale shear zone is to be expected. For example, it should be imaged in Lithoprobe deep-seismic experiment data (as predicted by Friedman and Armstrong, 1988). However, the current interpretation of most shallowly-dipping reflectors observed on the Southern Cordilleran Lithoprobe transect (about 250 km south-east) is as trans-Cordilleran thrust faults (Cook et al., 1992). Regional-scale detachment faults might also be imaged by confidential industry seismic data that has been recently re-processed (e.g., Hayward and Calvert, 2008) or by magnetotelluric data (e.g., Spratt and Craven, 2008), but in-

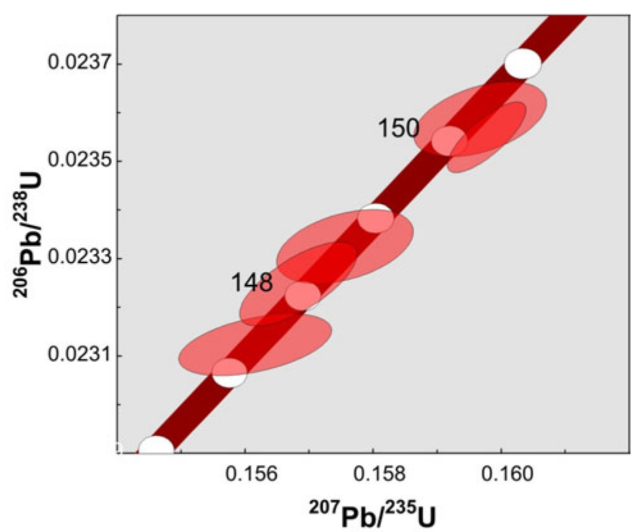

Figure 6. Concordia plots for U-Pb TIMS data for sample MMI07-33-3. The 2 error ellipses for individual analytical fractions are in red. Concordia bands include 2 errors on U decay constants.

Table 1. U-Pb thermal ionization mass spectrometry (TIMS) analytical data for zircon from sample MMI07-33-3, metadacite of the Dean River metamorphic belt.

Fraction[1]	Weight[2] (mg)	U^3 (ppm)	Pb^{*4} (ppm)	$^{206}Pb^5$/^{204}Pb	Pb^{*6}/Pbc	Pb^7 (pg)	Th-U[8]	Isotopic ratios ±1σ (%)[9] ^{206}Pb-^{238}U	±	^{207}Pb-^{235}U	±	^{207}Pb/^{206}Pb	±	corr. coeff.	%[10] discordant	Apparent ages ±2σ (Ma)[11] ^{206}Pb-^{238}U	±	^{207}Pb-^{235}U	±	^{207}Pb-^{206}Pb	±
Sample MMI07-33-3																					
A	8.1	712.0	17.6	6459	109.5	1.3	0.544	0.02355	0.13	0.1598	0	0.18787	0.05	0.779	5.0	150.0	0.4	150.5	0.4	157.8	4.6/4.6
B	7.7	308.0	7.5	3194	53.3	1.1	0.490	0.02359	0.13	0.1597	0	0.18783	0.09	0.440	1.5	150.3	0.4	150.4	0.7	152.6	11.1/11.2
C	5.5	389.0	9.5	3505	58.9	0.9	0.530	0.02325	0.15	0.1568	0	0.18767	0.05	0.707	-2.5	148.2	0.5	147.9	0.7	144.6	7.9/8.0
D	5.4	323.0	8.0	2787	48.0	0.9	0.583	0.02333	0.13	0.1576	0	0.18771	0.05	0.402	-0.8	148.6	0.4	148.6	0.8	147.5	11.8/11.9
E	5.0	307.0	7.4	1686	28.0	1.3	0.490	0.02312	0.11	0.1562	0	0.18493	0.13	0.466	-0.2	147.4	0.3	147.4	0.9	147.1	12.9/13.0

[1] All single grains, air-abraded.
[2] Grain mass determined on Sartorious SE2 ultra-microbalance to ±0.1 microgram.
[3] Corrected for spike, blank (0.2 pg ±50%, 2σ), and mass fractionation, which is directly determined with $^{233}U/^{235}U$ spike.
[4] Radiogenic Pb; data corrected for spike, fractionation, blank and initial common Pb; mass fractionation correction of 0.23% /amu ±40% (2σ) is based on analysis of NBS-982 throughout course of study; blank Pb correction of 0.5-1.0 pg ±40% (2σ) with composition of $^{206}Pb/^{204}Pb$ = 18.5 ±2%; $^{207}Pb/^{204}Pb$ = 15.5 ±2%; $^{208}Pb/^{204}Pb$ = 36.4 ±2%, all at 2σ; initial common Pb compositions based on the Stacey and Kramer (1975) model Pb at the interpreted age of the rock at 150 Ma.
[5] Measured ratio corrected for spike and fractionation.
[6] Ratio of radiogenic to common Pb.
[7] Total weight of common Pb calculated with blank isotopic composition.
[8] Model Th-U ratio calculated from radiogenic $^{208}Pb/^{206}Pb$ ratio and $^{207}Pb/^{206}Pb$ age.
[9] Corrected for spike, fractionation, blank and initial common Pb.
[10] Discordance in % to origin.
[11] Age calculations are based on decay constants of Jaffey et al., 1971.

terpretation and regional integration of these datasets are not yet complete. That a regionally-developed zone of Eocene detachment existed in the mid-crust seems necessary to explain normal faulting in central BC, which moderately tilts strata across tens of thousands of square kilometres (Lowe et al., 2001). Eocene crustal extension is also consistent with apatite and zircon fission track data from widespread localities that indicate rapid cooling between 55 and 50 Ma (Riddell et al., 2007). Breakaway zones, where ductile offset in the ductile mid-crust is transferred to the upper brittle crust through arrays of normal faults, are interpreted in the Puntzi Lake area (Mihalynuk et al., 2009) and may explain rapid lateral variations in Cretaceous and Tertiary Nechako Basin strata which appear as elongate sub-basins (e.g., as interpreted by Riddell et al., 2007).

Estimates of the structural omission across the main detachment zone can be deduced from the paleobarometric data in Friedman (1988). He shows an omission of roughly 13.5 km (~4.5 kbar); although at the limits of error for the geobarometers used, the thickness of missing crust ranges from ~3 to 24 km (~1–8 kbar). Closer to the central axis of the Intermontane Belt, minimum depth of any regional detachment fault is only constrained as >3778 m at the Chilcotin B-22-K hydrocarbon exploration well, about 80 km east-southeast of Rainbow Lake, which ends in undeformed volcanic rocks. Fifty kilometres south of the well, Tipper's Unit 4 metamorphic rocks are exposed at surface, requiring a regional dip on an interpreted single intervening detachment fault surface of more than 4.5 degrees.

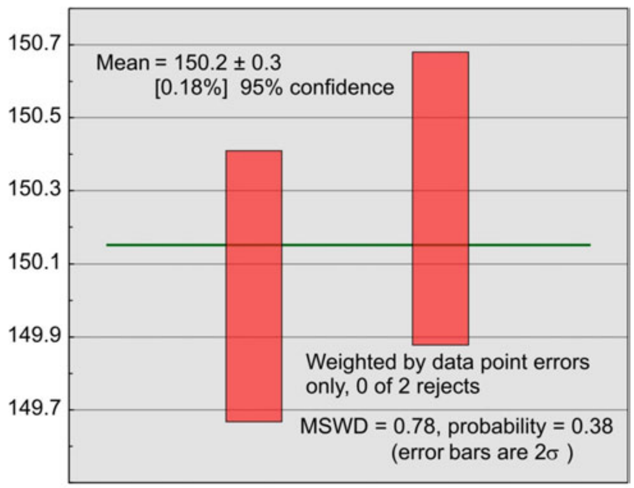

Figure 7. Mean square weighted deviates (MSWD) plot for the two most concordant fractions. Box heights are 2 .

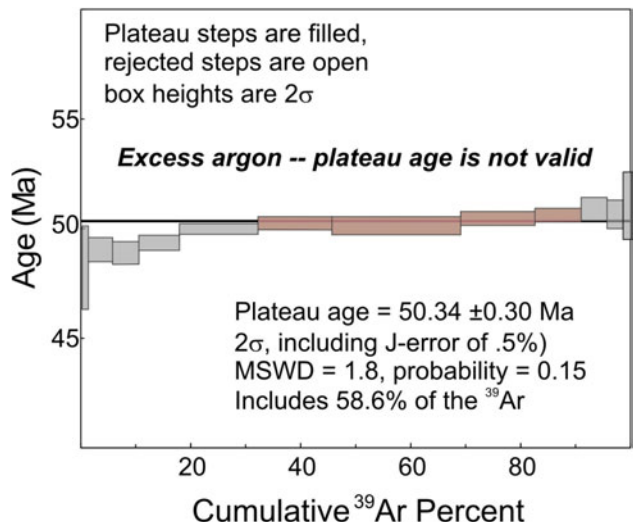

Figure 8. Step-heating Ar gas release spectra for sample MMI07-33-3. Rising steps indicate a problem with excess argon.

Table 2. $^{40}Ar/^{39}Ar$ step-heating gas release data from sample MMI07-33-3, metadacite of the Dean River metamorphic belt.

Laser Power (%)	Isotope Ratios $^{40}Ar/^{39}Ar$	$^{38}Ar/^{39}Ar$	$^{37}Ar/^{39}Ar$	$^{36}Ar/^{39}Ar$	Ca/K	Cl/K	$\%^{40}Ar$ atm	f ^{39}Ar	$^{40}Ar^*/^{39}ArK$	Age
Sample MMI07-33-3										
2	30.9386 ±0.0148	0.0498 ±0.0628	0.0391±0.1694	0.0683 ±0.0434	0.122	0.005	60.63	0.3	10.905 ±0.854	98.82 ±7.53
2.2	10.6132 ±0.0063	0.0226 ±0.0744	0.0272 ±0.1116	0.0183 ±0.0380	0.092	0.001	45.87	1.08	5.240 ±0.210	48.16 ±1.91
2.4	6.4570 ±0.0061	0.0148 ±0.0574	0.0518 ±0.0324	0.0038 ±0.0445	0.183	0	14.1	4.43	5.330 ±0.060	48.98 ±0.55
2.6	5.8561 ±0.0074	0.0132 ±0.0790	0.1303 ±0.0238	0.0018 ±0.0739	0.462	0	5.5	4.8	5.316 ±0.057	48.84 ±0.52
2.8	5.6854 ±0.0051	0.0132 ±0.0436	0.0205 ±0.0381	0.0010 ±0.0781	0.072	0	2.83	7.32	5.365 ±0.037	49.30 ±0.34
3	5.6263 ±0.0047	0.0124 ±0.0474	0.0104 ±0.0657	0.0005 ±0.0355	0.037	0	1.61	14.3	5.436 ±0.027	49.94 ±0.24
3.2	5.6253 ±0.0053	0.0122 ±0.0280	0.0084 ±0.0481	0.0004 ±0.1134	0.029	0	1.02	13.5	5.464 ±0.033	50.19 ±0.30
3.4	5.6025 ±0.0078	0.0122 ±0.0550	0.0062 ±0.0314	0.0004 ±0.1050	0.022	0	1.36	23.3	5.452 ±0.045	50.08 ±0.41
3.6	5.6857 ±0.0052	0.0122 ±0.0379	0.0070 ±0.0391	0.0006± 0.1129	0.025	0	1.65	13.5	5.489 ±0.035	50.42 ±0.32
3.8	5.8171 ±0.0053	0.0123 ±0.0410	0.0110 ±0.0278	0.0010 ±0.0533	0.038	0	2.85	8.31	5.507 ±0.034	50.58 ±0.31
4	5.9400 ±0.0086	0.0127 ±0.0953	0.0153 ±0.0888	0.0013 ±0.0790	0.053	0	2.95	4.72	5.537 ±0.059	50.85 ±0.53
4.2	6.1000 ±0.0080	0.0132 ±0.1530	0.0200 ±0.0706	0.0020 ±0.0931	0.07	0	4.13	2.96	5.510 ±0.072	50.61 ±0.65
4.4	6.4442 ±0.0103	0.0128 ±0.1512	0.0254 ±0.1070	0.0031 ±0.1744	0.088	0	4.35	1.56	5.554 ±0.170	51.00 ±1.54
Total/Average	*5.7405 ±0.0012*	*0.0126 ±0.0091*	*0.0347 ±0.0035*	*0.0008 ±0.0147*	*0.064*	*0*		*100*	*5.464 ±0.008*	

Notes
J = 0.005163 ±0.000012
Volume ^{39}ArK = 701.22
Integrated age = 50.19 ±0.18
Gas volume measurements to 10-13 cm^3 NPT
Neutron flux monitors: 28.02 Ma FCs (Renne et al., 1998)
Isotope production ratios: $(^{40}Ar/^{39}Ar)K$=0.0302 ±0.00006, $(^{37}Ar/^{39}Ar)Ca$=1416.4 ±0.5, $(^{36}Ar/^{39}Ar)Ca$=0.3952 ±0.0004, Ca/K=1.83 ±0.01 $(^{37}ArCa/^{39}ArK)$.

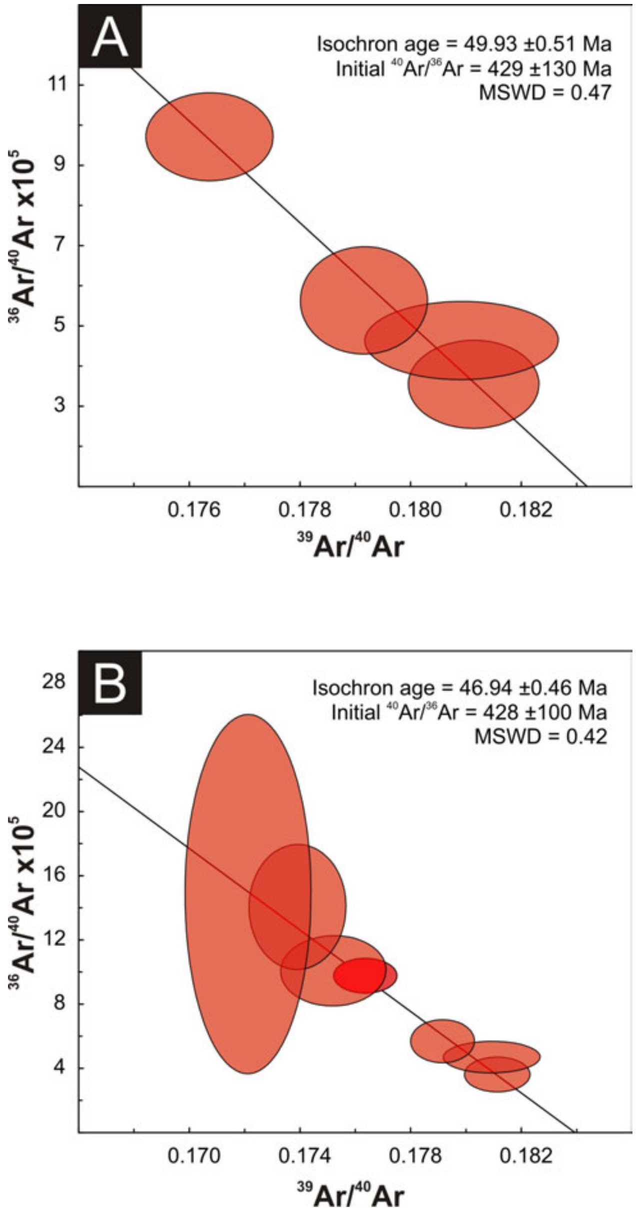

Figure 9. Ar isotope ratio correlation plots for **a)** plateau steps (N=4, *see* Figure 8), and **b)** plateau plus higher temperate steps (N=7). Both isochrons provide reliable age determinations which we report as 49.9 ±0.5 Ma.

Currently the crust within the Anahim Lake area is between 30 and 35 km thick as defined by the Mohorovicic discontinuity (Moho) extrapolated from the Lithoprobe transect (Cook et al., 1992) and as imaged in teleseismic data from the western Anahim Lake area. Preliminary interpretation of newly acquired teleseismic data from the Nechako Basin indicate a depth to the Moho of 35–40 km (J. Cassidy, personal communication, 2008), similar to the Moho depth near the eastern edge of the Coast Belt as imaged by Joshua Calkins et al. at the University of Arizona (*in* Cassidy and Al-Khoubbi, 2007; see their Figure 7). Including the omitted crustal section based upon the forgoing arguments, the pre-Eocene crust was probably in the order of 45–50 km thick (although post-Eocene cooling has probably depressed the Moho slightly).

Accuracy of models of the Eocene detachment surface, as well as thickness and composition of the crust affected by extension, are important considerations for resource assessment. Such considerations are especially germane for petroleum source-rock potential as the shallow crust may have been translated tens of kilometres by detachment, and rocks below any detachment fault are likely to have been subjected to significantly higher temperatures and pressures than those in the immediate hangingwall. Additionally, in the southwest United States, detachment faults are recognized as principal control on one group of polymetallic (Cu-Au-Ag-Pb-Zn) deposits. The detachment fault-related polymetallic deposit model (Wilkins et al., 1986) is a largely unexplored deposit type in BC. Small, scattered copper showings in the metamorphic rocks in southeastern Anahim Lake map area (Mihalynuk et al., 2009) may be an early indication of the exploration opportunities that exist for this type of mineralization, especially if the Tatla Lake metamorphic complex is part of a much more regional detachment system.

ACKNOWLEDGMENTS

T. Ullrich processed the $^{40}Ar/^{39}Ar$ samples and generated the step release data, spectra and inverse isochron plots. L. Diakow conscientiously reviewed an earlier draft of this paper. J. Cassidy kindly offered advice based upon the most recently available teleseismic data. Assistance with mineral separation and mass spectrometry was provided by H. Lin; Y. Feng helped with grain selection, pretreatment and sample dissolution/processing.

REFERENCES

BC Ministry of Forests and Range (2005): The state of British Columbia's forests 2004; *BC Ministry of Forests and Range*, URL< http://www.for.gov.bc.ca/hfp/sof/2004/> [November 2007].

Cassidy, J. and Al-Khoubbi, I. (2007): A passive seismic investigation of the geological structure within the Nechako Basin; *in* The Nechako Initiative—Geoscience Update, *BC Ministry of Energy, Mines and Petroleum Resources*, Petroleum Geology Open File 2007-1 pages 7–57, URL <http://www.empr.gov.bc.ca/OG/oilandgas/petroleumgeology/CoventionalOilAndGas/InteriorBasins/Documents/The_Nechako_Initiative-Geoscience_Update_2007.pdf> [November 2008].

Cassidy, J.F., Al-Khoubbi, I. and Kim, H.S. (2008): Mapping the structure of the Nechako Basin using passive source seismology; *in* Geoscience BC Summary of Activities 2007, *Geoscience BC*, Report 2008-1, pages 115–120.

Cook, F.A., Varsek, J.L., Clowes, R.M., Kanasewich, E.R., Spencer, C.S., Parrish, R.R. Brown, R.L., Carr, S.D., Johnson, B.J. and Price, R.A. (1992): LITHOPROBE crustal reflection structure of the southern Canadian Cordillera 1, foreland thrust and fold belt to Fraser River fault; *Tectonics*, Volume 11, pages 12–35.

Friedman, R.M. (1988): Geology and geochronology of the Eocene Tatla Lake Metamorphic Core Complex, western edge of the Intermontane Belt, British Columbia; Ph.D. thesis, *University of British Columbia*, 348 pages.

Friedman, R.M. and Armstrong, R.L. (1988): Tatla Lake metamorphic complex: an Eocene metamorphic core complex on the southwestern edge of the Intermontane Belt of British Columbia; *Tectonics*, Volume 7, pages 1141–1166.

Friedman, R.M. (1992): P-T-t path for the lower plate of the Eocene Tatla Lake metamorphic core complex, southwestern Intermontane Belt, British Columbia; *Canadian Journal of Earth Sciences*, Volume 29, pages 972–983.

Hayward, N. and Calvert, A.J. (2008): Structure of the south eastern Nechako Basin, south-central British Columbia (NTS 092N, O; 093B, C): preliminary results of seismic interpretation and first-arrival tomographic modelling; *in* Geoscience BC Summary of Activities 2007, *Geoscience BC*, Report 2008-1, pages 129–134.

Jaffey, A.H., Flynn, K.F., Glendenin, L.E., Bentley, W.C., Essling, A.M. (1971): Precision measurement of half-lives and specific activities of ^{235}U and ^{238}U; *Physical Review C*, Volume 4, pages 1889–1906.

Logan, J.M., Mihalynuk, M.G., Ullrich, T. and Friedman, R.M. (2007): U-Pb ages of intrusive rocks and ^{40}Ar/^{39}Ar plateau ages of copper-gold-silver mineralization associated with alkaline intrusive centres at Mount Polley and the Iron Mask batholith, southern and central British Columbia; *in* Geological Fieldwork 2006, *BC Ministry of Energy, Mines and Petroleum Resources*, Paper 2007-1, pages 93–116, URL <http://www.em.gov.bc.ca/DL/GSBPubs/GeoFldWk/2006/11-Logan.pdf> [November 2008].

Lowe, C., Enkin, R.J. and Struik, L.C. (2001): Tertiary extension in the central British Columbia Intermontane Belt: magnetic and paleomagnetic evidence from the Endako region; *Canadian Journal of Earth Sciences*, Volume 38, pages 657–678.

Mattinson, J.M. (2005): Zircon U-Pb chemical abrasion ("CA-TIMS") method: combined annealing and multi-step partial dissolution analysis for improved precision and accuracy of zircon ages; *Chemical Geology*, Volume 220, pages 47–66.

Mihalynuk, M.G. (2007a): Evaluation of mineral inventories and mineral exploration deficit of the Interior Plateau Beetle Infested Zone (BIZ); *in* Geological Fieldwork 2006, *BC Ministry of Energy, Mines and Petroleum Resources*, Paper 2007-1, pages 137–142, URL <http://www.em.gov.bc.ca/DL/GSBPubs/GeoFldWk/2006/14-Mihalynuk.pdf> [November 2007].

Mihalynuk, M.G. (2007b): Neogene and Quaternary Chilcotin Group cover rocks in the Interior Plateau, south-central British Columbia: a preliminary 3-D thickness model; *in* Geological Fieldwork, *BC Ministry of Energy, Mines and Petroleum Resources*, Paper 2007-1, pages 143–147, URL <http://www.em.gov.bc.ca/DL/GSBPubs/GeoFldWk/2006/15-Mihalynuk.pdf> [November 2007].

Mihalynuk, M.G., Erdmer, P., Ghent, E.D., Cordey, F., Archibald, D.A., Fried man, R.M. and Johannson, G.G. (2004): Coherent French Range blueschist: subduction to exhumation in <2.5 m.y.?; *Bulletin of the Geological Society of America*, Volume 116, pages 910–922.

Mihalynuk, M.G., Harker, L.L., Lett, R. and Grant, B. (2007): Results of reconnaissance surveys in the Interior Plateau Beetle Infested Zone (BIZ); *BC Ministry of Energy, Mines and Petroleum Resources*, GeoFile 2007-5, URL <http://www.empr.gov.bc.ca/Mining/Geoscience/PublicationsCatalogue/GeoFiles/Pages/2007-5.aspx> [November 2007].

Mihalynuk, M.G., Peat, C.R., Terhune, K. and Orovan, E.A. (2008): Regional geology and re source potential of the Chezacut map area, central British Columbia (NTS 093C/08); *in* Geological Fieldwork 2007, *BC Ministry of Energy, Mines and Petroleum Resources,* Paper 2008-1, pages 117–134, URL <http://www.em.gov.bc.ca/DL/GSBPubs/GeoFldWk/2007/13-Mihalynuk-Chezacut34526.pdf> [November 2008].

Mihalynuk, M.G., Orovan, E.A., Larocque, J.P., Friedman, R.M. and Bachiu, T. (2009): Geology, geochronology and mineralization of the Chilanko Forks to southern Clusko River area, British Columbia (NTS 93C/01, 08, 09S); *in* Geological Fieldwork 2008, *BC Ministry of Energy, Mines and Petroleum Resources*, Paper 2009-1, pages 81–100.

MINFILE (2008): MINFILE BC mineral deposits database; *BC Ministry of Energy, Mines and Petroleum Resources*, URL <http://www.minfile.ca> [November 2008].

Mundil, R., Ludwig, K.R., Metcalfe, I. and Renne, P.R. (2004): Age and timing of the Permian mass extinctions: U/Pb dating of closed-system zircons; *Science*, Volume 305, pages 1760–1763.

Renne, P.R., Swisher, C.C., III, Deino, A.L., Karner, D.B., Owens,T. and DePaolo, D.J. (1998): Intercalibration of standards, absolute ages and uncertainties in ^{40}Ar/^{39}Ar dating; *Chemical Geology*, Volume 145, Numbers 1–2, pages 117–152.

Riddell, J.M., Ferri, F., Sweet, A.R. and O'Sullivan, P.B. (2007): New geoscience data from the Nechako Basin project; *in* The Nechako Initiative—Geoscience Update 2007, *BC Ministry of Energy, Mines and Petroleum Resources*, Petroleum Geology Open File 2007-1, pages 59–98, URL <http://www.empr.gov.bc.ca/OG/oilandgas/petroleumgeology/ConventionalOilAndGas/InteriorBasins/Documents/The_Nechako_Initiative-Geoscience_Update_2007.pdf> [November 2008].

Schiarizza, P., Panteleyev, A., Gaba, R.G., Glover, J.K. (1994): Geological compilation of the Cariboo-Chilcotin area, south-central British Columbia (NTS 92J, K, N, O, P; 93A, B, C, F, G, H); *BC Ministry of Energy, Mines and Petroleum Resources*, Open File 1994-7, scale 1:250 000, URL <http://www.empr.gov.bc.ca/Mining/Geoscience/PublicationsCatalogue/OpenFiles/1994/Pages/1994-7.aspx> [November 2008].

Souther, J.G. and Souther, M.E.K. (1994): Geology, Ilgachuz Range and adjacent parts of the Interior Plateau, British Columbia; *Geological Survey of Canada*, Map 1845A, scale 1:50 000.

Spratt, J. and Craven, J. (2008): A first look at the electrical resistivity structure in the Nechako Basin from magnetotelluric studies west of Nazko, British Columbia (NTS 092 N, O; 093 B, C, F, G); Geoscience Reports 2008, *BC Ministry of Energy, Mines and Petroleum Resources*, pages 119–127.

Stacey, J.S., Kramer, J.D. (1975): Approximation of terrestrial lead isotope evolution by a two-stage model; *Earth and Planetary Science Letters*, Volume 26, pages 207-221.

Struik, L.C. (1993): Intersecting intracontinental Tertiary transform fault systems in the North American Cordillera; *Canadian Journal of Earth Sciences*, Volume 30, pages 1262–1274.

Tipper, H.W. (1969): Geology, Anahim Lake; *Geological Survey of Canada*, Map 1202A, scale 1:253 440.

Wilkins, Joe, Jr., Beane, R.E., and Heidrick, T.L., 1986, Mineralization related to detachment faults: a model; *in* Frontiers in Geology and Ore Deposits of Arizona and the Southwest, Beatty, B. and Wilkinson, P.A.K., Editors, *Arizona Geological Society Digest*, Volume 16, pages 108–117.